Understanding comb formation in microrings

Roman Shugayev

Experimental observation of frequency combs

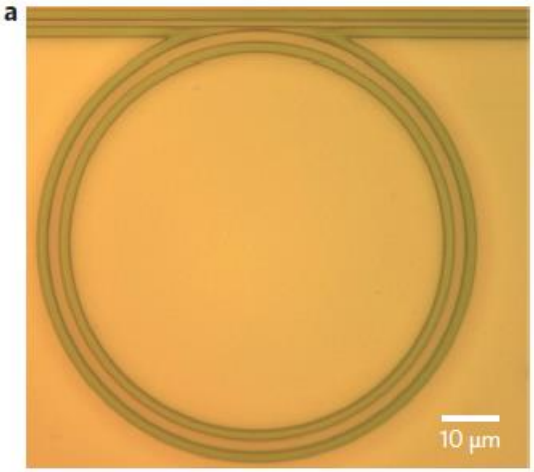

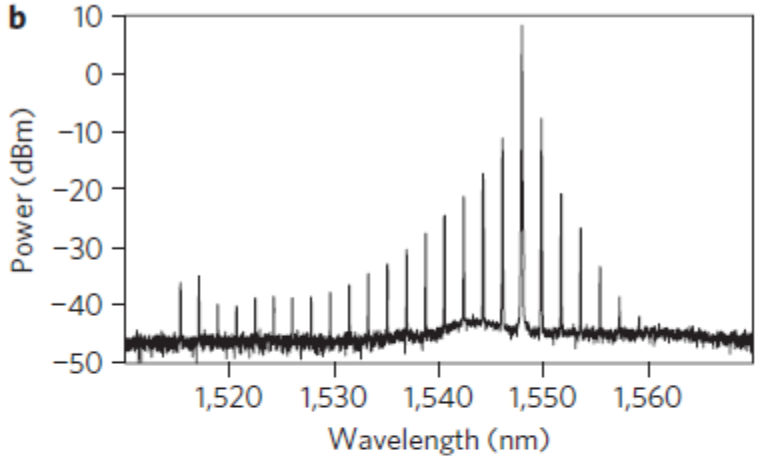

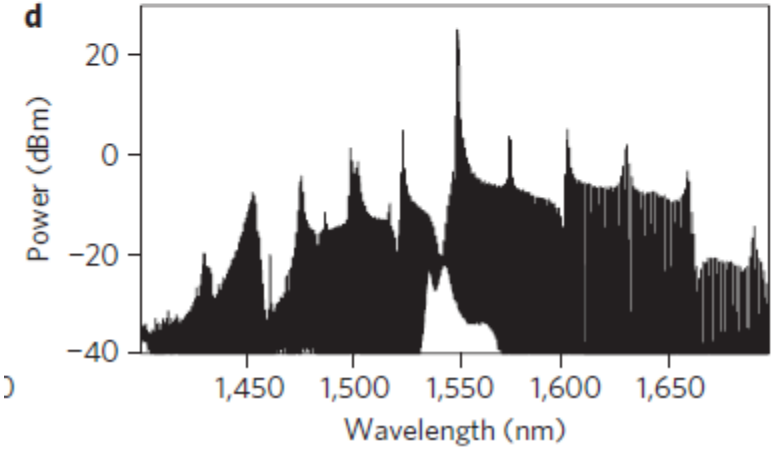

F. Ferdous et al. ” Spectral line-by-line pulse shaping of on-chip microresonator frequency combs,” Nature Photon. 5, 770-776 (2011).

Four-wave mixing in the micoresonators

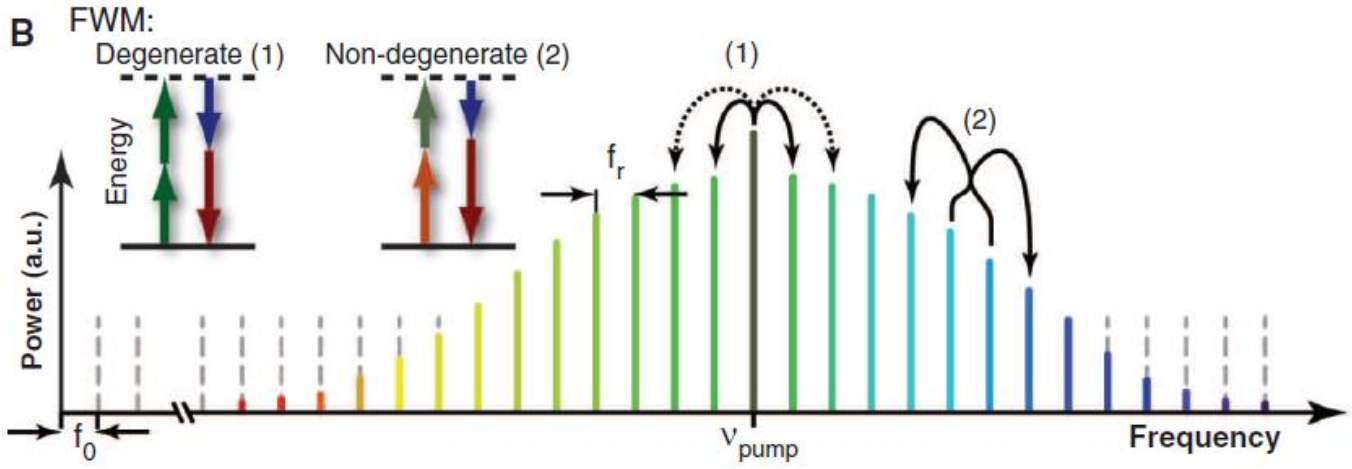

Kippenberg et al. “Microresonator-Based Optical Frequency Combs,” Science 332, 555-559 (2011).

Type I/II comb formation

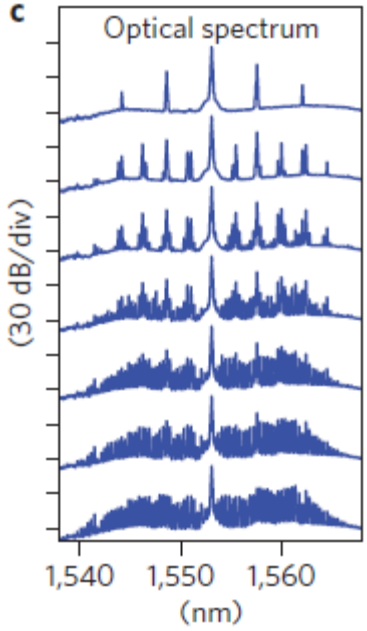

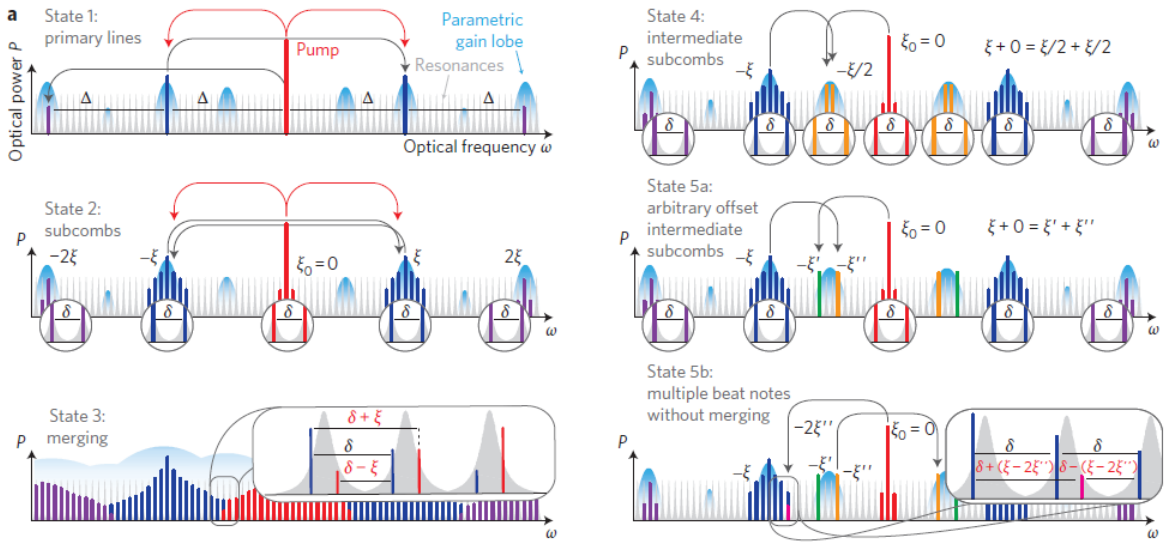

T. Herr et al. "Universal formation dynamics and noise of Kerr-frequency combs in microresonators" Nature Photon. 6, 480-7 (2012).

$$\omega_n^i = \omega_p + \xi_i + n\sigma, \quad n = 0, \pm 1, \pm 2 \ldots$$

Quadratures. Example

$$v = L\frac{di}{dt}$$

$$i = -C\frac{dv}{dt}$$

$$U = \frac{CV^2}{2} + \frac{LI^2}{2}$$

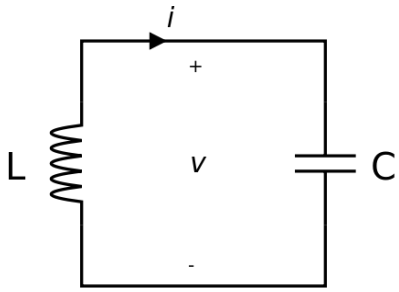

$$\frac{d^2v}{dt^2} + \omega_0^2 v = 0 \qquad \omega_0^2 = \frac{1}{LC}$$

Coupled second order differential equation

$$a_{\pm} = \sqrt{\frac{C}{2}}\left(v \pm j\sqrt{\frac{L}{C}}i\right)$$

Defining the quadrature operators

$$\frac{da_+}{dt} = j\omega_0 a_+$$

$$\frac{da_-}{dt} = -j\omega_0 a_-$$

System has been decoupled

Coupled mode theory

CMT –system of coupled differential equations subject to Kerr nonlinearity and external source excitation

$$\frac{da_i}{dt} = -i\omega_i a_i + iK_{ijkl} e^{i(\omega_k + \omega_l - \omega_i - \omega_j)t} a_j^{\dagger} a_k a_l + s^{+}$$

$a_i \quad a_i^{\dagger}$ Are creation and annihilation operators (normalized to energy)

K_{ijkl} Coupling coefficient

s^{+} Input amplitude (normalized to power)

Determining coupling coefficient

$$\mathrm{H} = \frac{1}{2}\int dr\left[\varepsilon E(r)^2 + \frac{1}{\mu}B(r)^2\right]$$ Total Energy

$$\varepsilon(r,t) = \varepsilon_0(r) + \varepsilon_2\left|E(r)\right|^2$$ Permittivity

Assuming that the fields can be written as
a sum of second quantized operators for for the plane waves

$$E(r) = \sum_k \sqrt{\frac{\hbar\omega_k}{2V\varepsilon_0}} e^{ikr}\left[a_k + a_k^\dagger\right]\hat{x}$$

$$B(r) = i\sum_k |k| \sqrt{\frac{\hbar}{2V\varepsilon_0\omega_k}} e^{ikr}\left[a_k - a_k^\dagger\right]$$

We can normalize the energy to $\hbar\omega$
Appling Heizenberg equation of motion :

$$\frac{da_i}{dt} = \frac{1}{i\hbar}\left[a_i, H\right]$$

$$\frac{da_i}{dt} = -i\omega_i a_i + iK_{ijkl} e^{i(\omega_k+\omega_l-\omega_i-\omega_j)t} a_j^\dagger a_k a_l$$

Coupling coefficient for arbitrary field distribution

$$E = k \cdot g(r)(a_k + a_k^\dagger)$$

$g(r)$ is a normalized modal field distribution

$$H = k^2 \int \varepsilon(r) g(r)^2 (a_k + a_k^\dagger)^2 dr$$

$$H = 2 a_k a_k^\dagger k^2 \int \varepsilon_k(r) g_k(r)^2 dr = \hbar \omega_k a_k a_k^\dagger$$

$$k = \sqrt{\frac{\hbar \omega}{2 \int \varepsilon_k(r) g_k(r)^2 dr}}$$

$$K_{ijkl} = \frac{\hbar \varepsilon_2}{8} \sqrt{\omega_i \omega_j \omega_k \omega_l} \frac{\int g_i(r) g_j(r) g_k(r) g_l(r) dr}{\left(\int \varepsilon_i(r) g_i(r)^2 dr \int \varepsilon_j g_j(r)^2 dr \int \varepsilon_k g_k(r)^2 dr \int \varepsilon_l g_l(r)^2 dr \right)^{1/2}}$$

Applying formalism to microring system

- Mode distribution (Bessel function)
- Different families have different dispersion signs

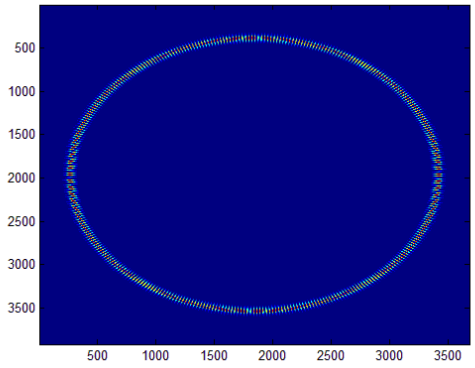

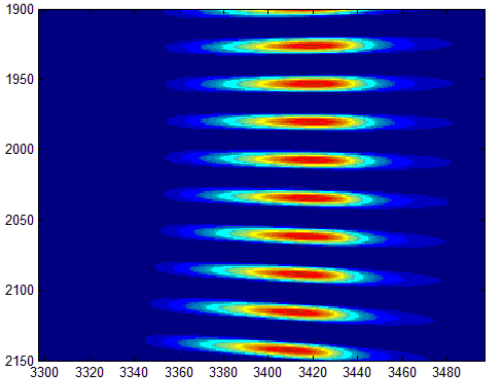

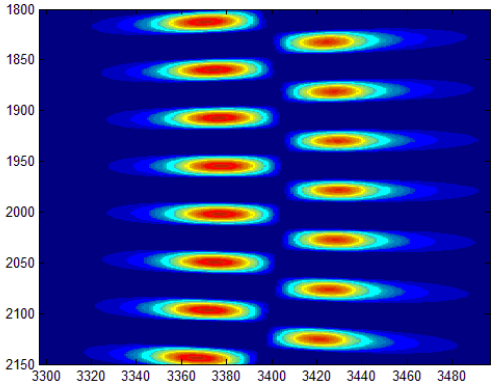

Comparing results. Normal dispersion

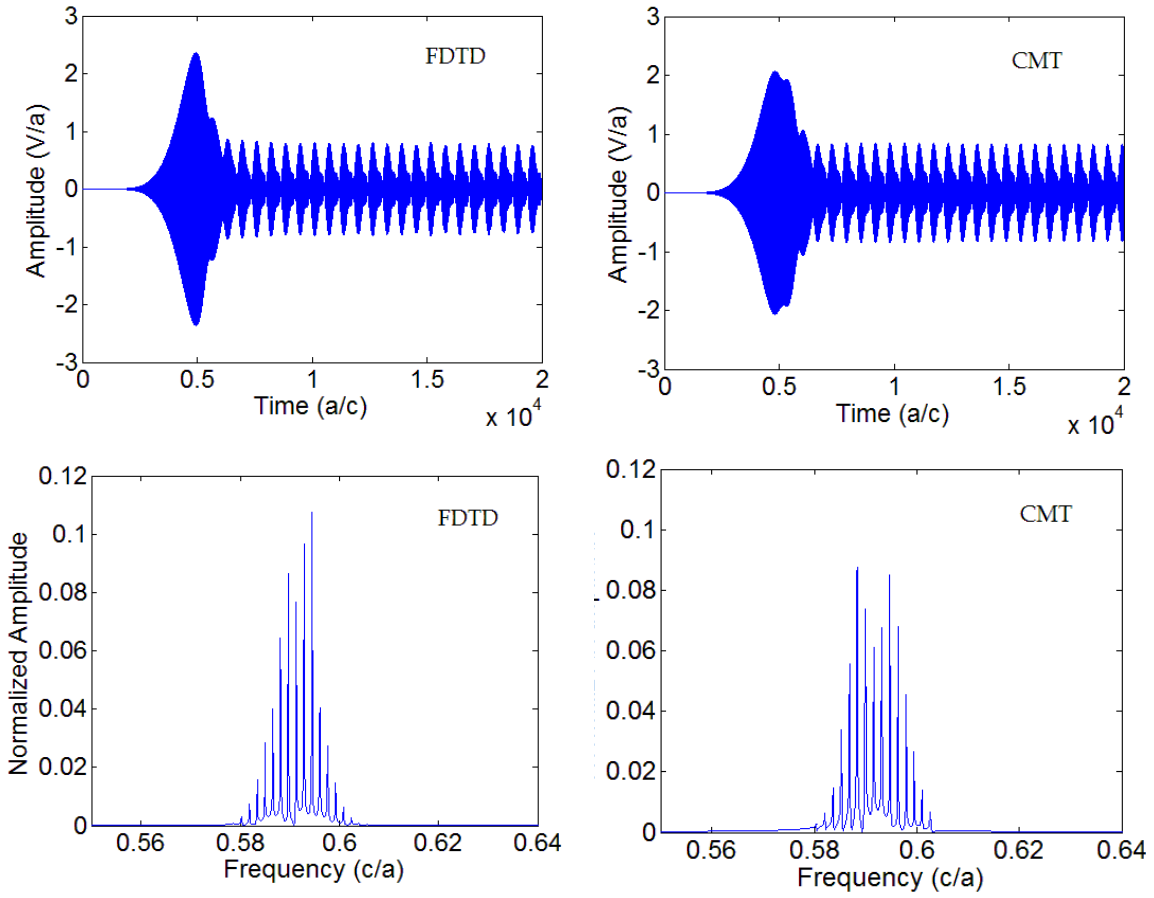

Comparing results. Anomalous dispersion

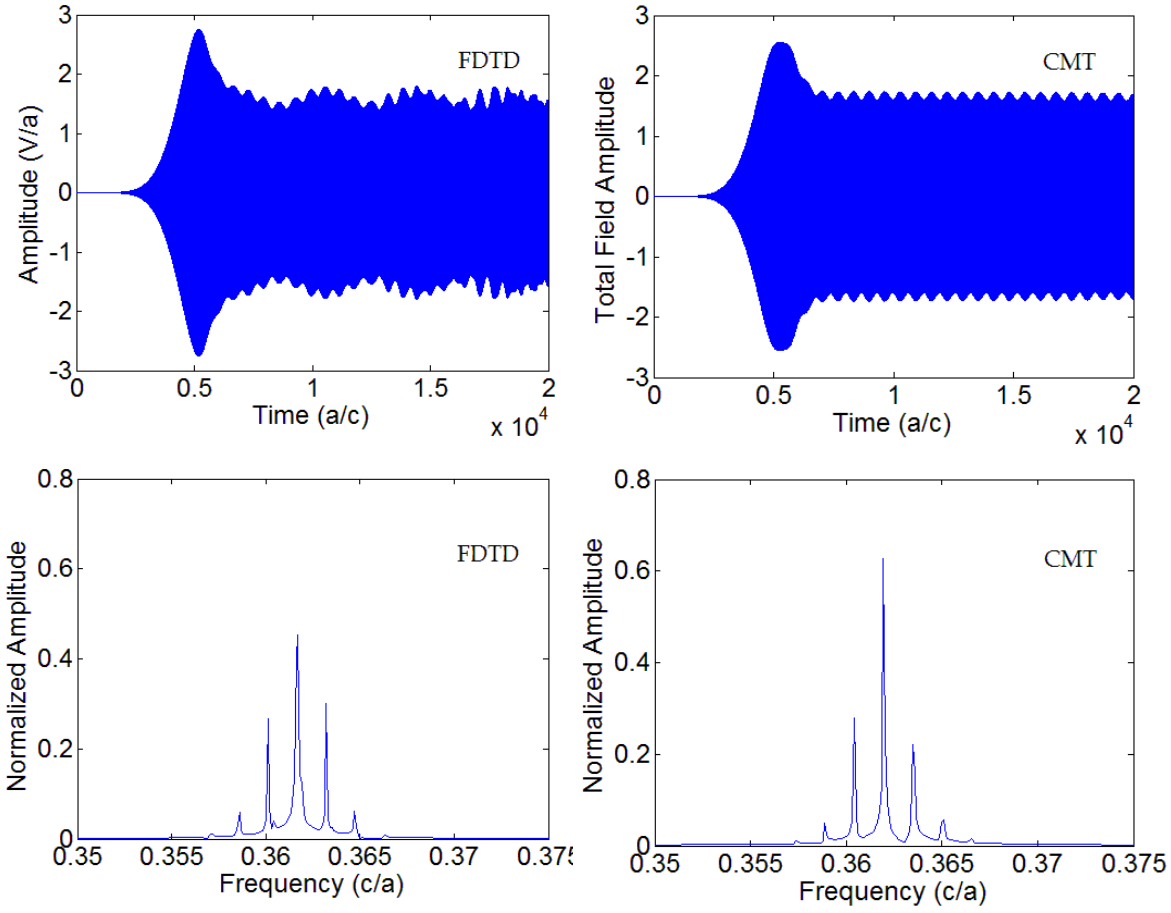

Gaining insight into comb formation

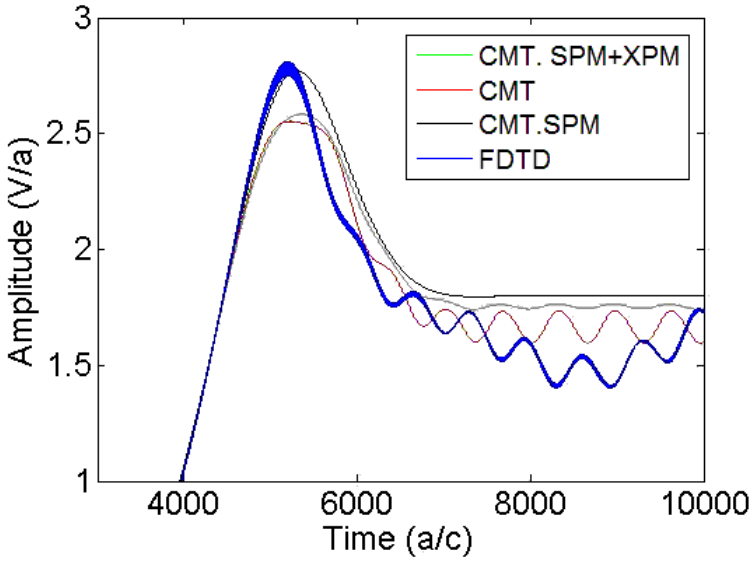

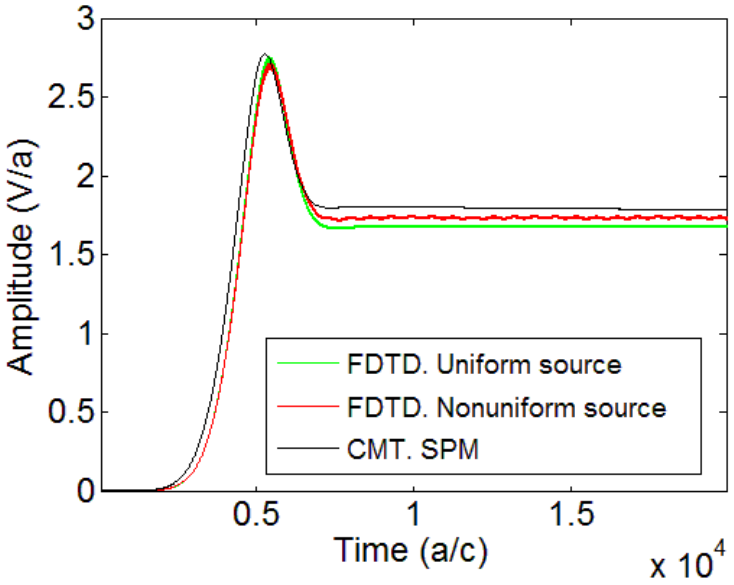

SPM XPM

$$\frac{da_s}{dt} = i\left\{\omega a_s + |a_s|^2 a_s + 2a_s\left(|a_p|^2 + |a_i|^2\right) + a_p^2 a_i^*\right\}$$

$$\frac{da_p}{dt} = i\left\{\omega a_p + |a_p|^2 a_p + 2a_p\left(|a_s|^2 + |a_i|^2\right) + a_i a_s a_p^*\right\}$$

$$\frac{da_p}{dt} = i\left\{\omega a_i + |a_i|^2 a_i + 2a_i\left(|a_p|^2 + |a_s|^2\right) + a_p^2 a_s^*\right\}$$

- Self phase modulation (SPM) mimics initial pulse transient
- Conclusion: Cross-phase modulation (XPM) in the initial phase of the pulse formation is not present Why?

Origins of absence of coupling
Symmetry breaking

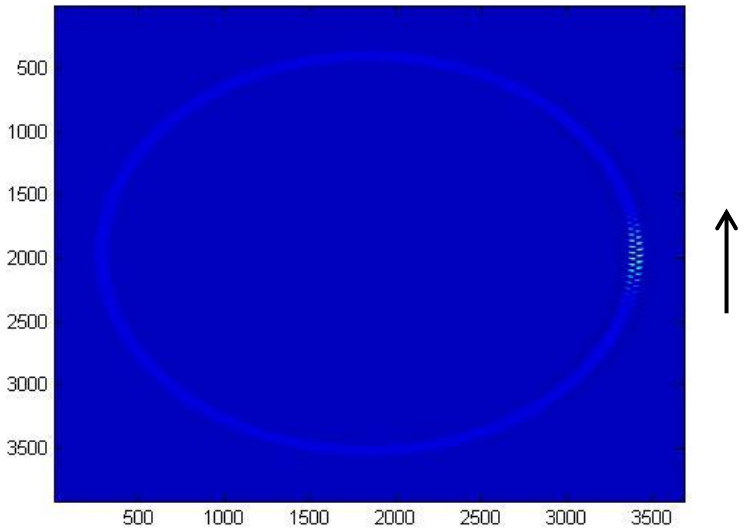

$$\frac{da_i}{dt} = i\left\{\omega_i a_i + |a_i|^2 a_i\right\}$$

$$\frac{da_i}{dt} = i\left\{\omega_i a_i + |a_i(r)|^2 a_i\right\}$$

- Modes have a localized traveling profile and hence no overlap to produce cross-phase modulation or energy transfer

Soliton propagation in FDTD and CMT

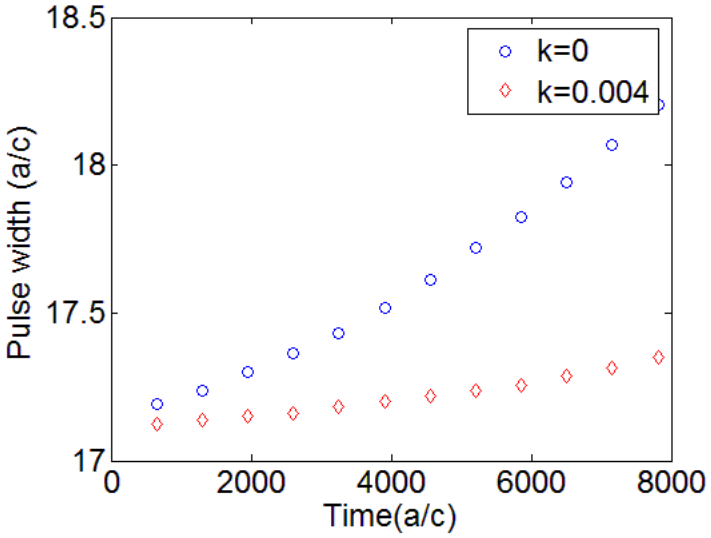

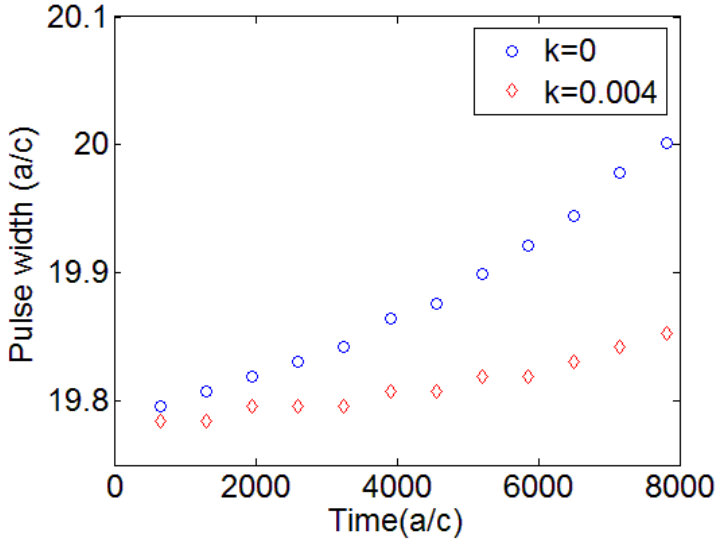

- Pulse spreading is reduced from FDTD to CMT since we only considered N=29 modes

Further Applications. Random lasers

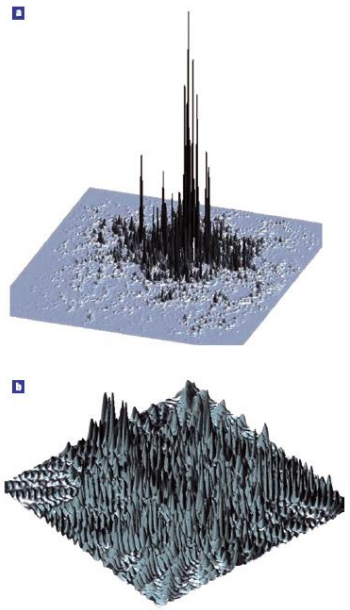

Figure 3 Extended versus localized optical modes. Finite-difference time-domain calculation of the distribution of the electromagnetic-field intensity in a disordered system. **a**, A localized mode. Here, the light is confined to a mode with exponentially decaying tails. **b**, An extended mode. The strongly fluctuating pattern is called speckle. The calculation is carried out for a 2D planar waveguide with random pores. A similar pattern can be expected inside 3D random materials.

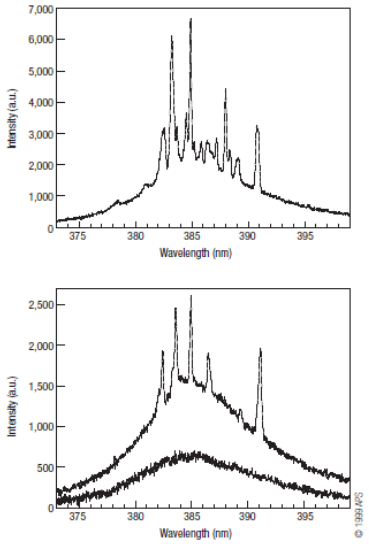

Figure 4 Complex emission spectra exhibiting narrow spikes. Emission spectra of a random laser exhibiting an overall narrowing of the spectrum together with narrow spikes at random frequencies. The sample consists of zinc oxide powder with grain size of the order of 100 nm and is excited by laser pulses of 15 ps pulse duration at 355 nm wavelength (excitation area from bottom to top: 980, 1,350 and 1,870 mm²). Reprinted with permission from ref. 23.

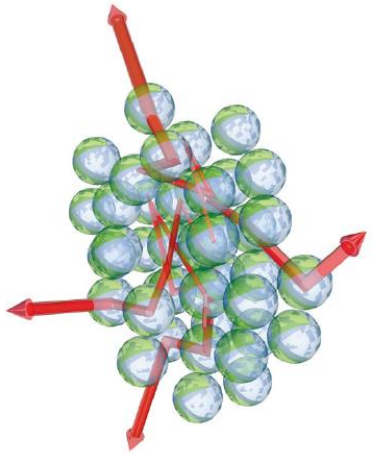

Figure 1 Multiple light scattering with gain. A random collection of microspheres containing laser dye is excited (for example, by an external light source) to obtain population inversion. The microspheres then scatter light and amplify it in the process. The propagation of the light waves becomes that of an amplified random walk.

Wiersma , *Nature Physics*, **4** (2008) (Review article)

Random lasers. Recent developments

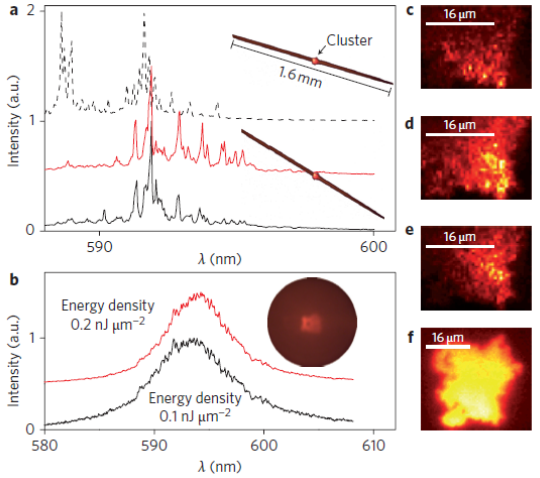

Figure 1 | The two random lasing regimes. a, Three normalized spectra, each obtained by averaging 100 single shots from pumping a stripe-shaped area (length, 1.6 mm). Top and bottom traces were retrieved for a stripe of the same thickness (16 μm), but with different orientations (15° tilt). The middle trace is for a stripe with the same orientation as for the bottom trace, but with twice the thickness. **b**, Spectrum for disk-shaped pumping (diameter, 1 mm) for two different pump densities. The insets show sketches of the pumping areas. **c**-**f**, Emitted intensity distributions corresponding to the lines in **a** and **b**. Scale bars, 16 μm. Images were retrieved by optical imaging of the RL emission obtained with a pumping fluence of 0.1 nJ μm^{-2}.

Leonetti et al, *Nature Photonics* **5** (2011)

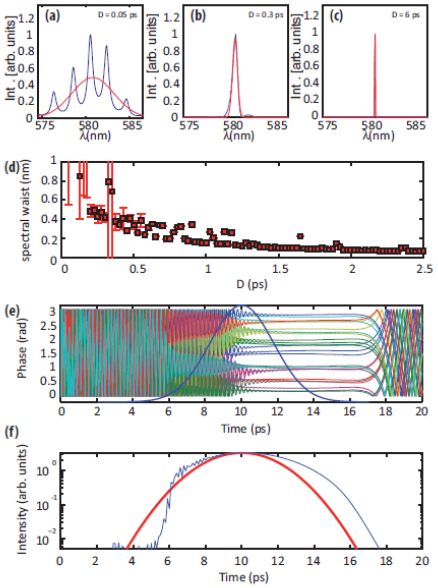

FIG. 5. (Color online) Results of the numerical simulations. (a–c) The spectra obtained for various pumping durations. (d) The spectral waist retrieved by Gaussian fitting (red line in the first three panels) as a function of the pumping duration D. (e, f) The phases and the total intensity, respectively, as a function of time. The pump pulse shape ($D = 2.5$ ps) is represented as a thick line.

Leonetti et al, *PHYSICAL REVIEW A* **88**, 043834 (2013)

Framework of CMT:

$$\frac{da_i(t)}{dt} = i\omega_i a_i(t) - \alpha_i a_i(t) + \sum_{\text{neighbors}} C_{ij} a_j(t) + \frac{G(t) a_i(t)}{1 + \gamma |a_i|^2}$$

Q&A